We are IntechOpen, the world's leading publisher of Open Access books
Built by scientists, for scientists

6,900
Open access books available

185,000
International authors and editors

200M
Downloads

154
Countries delivered to

Our authors are among the
TOP 1%
most cited scientists

12.2%
Contributors from top 500 universities

CLARIVATE ANALYTICS
BOOK CITATION INDEX
INDEXED

WEB OF SCIENCE™

Selection of our books indexed in the Book Citation Index
in Web of Science™ Core Collection (BKCI)

Interested in publishing with us?
Contact book.department@intechopen.com

Numbers displayed above are based on latest data collected.
For more information visit www.intechopen.com

Aircraft Gas-Turbine Engine's
Control Based on the Fuel Injection Control

Alexandru-Nicolae Tudosie
University of Craiova, Avionics Department
Romania

1. Introduction

For a gas-turbine engine, particularly for a jet engine, the automatic control is one of the most important aspects, in order to assure to it, as aircraft's main part, an appropriate operational safety and highest reliability; some specific hydro-mechanical or electro-mechanical controller currently realizes this purpose.

Jet engines for aircraft are built in a large range of performances and types (single spool, two spools or multiple spools, single jet or twin jet, with constant or with variable exhaust nozzle's geometry, with or without afterburning), depending on their specific tasks (engines for civil or for combat aircraft). Whatever the engine's constructive solution might be, it is compulsory that an automatic control system assist it, in order to achieve the desired performance and safety level, for any flight regime (altitude and speed).

Regarding the nowadays aircraft engine, the more complex their constructive solution is, the bigger the number of their parameters is. Considering an engine as a controlled object (see figure 1.a), one has to identify among these parameters the most important of them, the easiest to be measured and, in the mean time, to separate them in two classes: control parameters and controlled parameters. There is a multitude of eligible controlled parameters (output parameters, such as: thrust, fuel consumption, spool(s) speed, combustor's temperature etc.), but only a few eligible control parameters (input parameters, such as: fuel flow rate, nozzle's exit area and/or inlet's area). It results a great number of possible combinations of control programs (command laws) connecting the input and the output parameters, in order to make the engine a safe-operating aircraft part; for a human user (a pilot) it is impossible to assure an appropriate co-ordination of these multiples command laws, so it is compulsory to use some specific automatic control systems (controllers) to keep the output parameters in the desired range, whatever the flight conditions are.
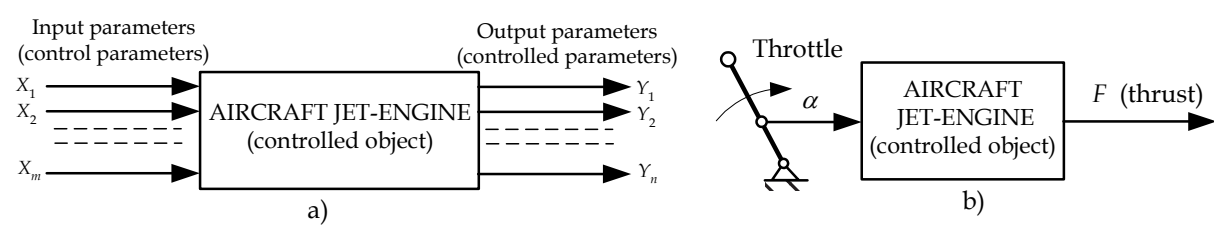

Fig. 1. Aircraft engines as controlled objects

In fact, the pilot has only a single engine's command possibility, a single input parameter - the throttle displacement and a single relevant output parameter – the engine's thrust (as shown in figure 1.b). Although, the engine's thrust is difficult to be measured and displayed, but it could be estimated and expressed by other parameters, such as engine's spool(s) speed(s) or gas temperature behind the turbine, which are measured and displayed much easier.

Consequently, most of aircraft engine command laws and programs are using as control parameters the fuel flow rate Q_c (which is the most important and the most used) and the exhaust nozzle throat and/or exit area A_5 and as controlled parameters the engine's spool (s) speed(s) and/or the engine's exhaust burned gas temperature. Meanwhile, in an engine control scheme, throttle's displacement becomes itself the input for a mixed (complex) setting block, which establishes the reference parameters for the engine's controller(s), as shown in figure 2. So, in this case, both engine's control parameters become themselves controlled parameters of the engine's controller(s), a complex engine control system having as sub-systems an exhaust nozzle exit area control system (Aron & Tudosie, 2001) as well as a fuel injection control system (Lungu & Tudosie, 1997).

Because of the fuel injection great importance, fuel injection controllers' issue is the main concern for pump designers and manufacturers.
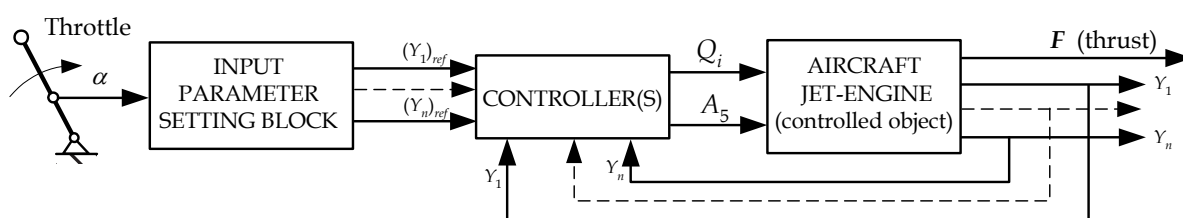

Fig. 2. Aircraft engine's automatic control system

2. Principles of the fuel flow rate control

Aircraft engines' fuel supply is assured by different type of pumps: with plungers, with pinions (toothed wheels), or with impeller. For all of them, the output fuel flow rate depends on their rotor speed and on their actuator's position; for the pump with plungers the actuator gives the plate's cline angle, but for the other pump type the actuator determines the by-pass slide-valve position (which gives the size of the discharge orifice and consequently the amount of the discharged fuel flow rate, as well as the fuel pressure).

The fuel flow rate through some injection scheme part (x) Q_x is given by the generic formula (where μ_x is the x-part flow co-efficient, depending on its inner channel shape and roughness, A_x – x-part injection effective area, ρ – fuel density, p_b – pressure before and p_a – pressure after the above-mentioned part):

$$Q_x = \mu_x A_x \sqrt{\frac{2}{\rho}} \sqrt{p_b - p_a} \, . \tag{1}$$

Consequently, the fuel flow rate through the injector(s) is

$$Q_i = \mu_i A_i \sqrt{\frac{2}{\rho}} \sqrt{p_i - p_{CA}} \, , \tag{2}$$

and through the dosage valve (before the injector) is, similarly,

$$Q_d = \mu_d A_d \sqrt{\frac{2}{\rho}} \sqrt{p_p - p_i} \, , \tag{3}$$

where μ_i and μ_r are the flow co-efficient, p_i – fuel injection pressure, p_{CA} – air/gases pressure in the engine's combustor, p_p – fuel pump supplying pressure, A_d – dosage valve's effective area (depending on the pump's actuator displacement), A_i – injector's effective area, assumed as circular $\left(A_i = \dfrac{\pi d_i^2}{4} \right)$, d_i – injector's diameter.

For a steady state regime the fuel flow rate is constant, so $Q_i = Q_r$, which leads to a new expression for the injected flow rate (Stoenciu, 1986), where $f = \dfrac{\mu_i A_i}{\mu_d A_d}$:

$$Q_r = \mu_d A_d \sqrt{\frac{2}{\rho(1+f)}} \sqrt{p_p - p_{CA}} \, . \tag{4}$$

As far as, for a constant engine operating regime p_{CA} can be assumed as constant, the fuel flow rate depends on p_p (or $p_p - p_i$) and A_r, therefore a fuel flow rate controller has to deal with one of these parameters, or with both of them simultaneously.

Nowadays common use basic fuel injection controllers are built, according to this observation, as following types (Stoicescu & Rotaru, 1999):
- with constant fuel pressure and adjustable fuel dosage valve;
- with constant fuel differential pressure and adjustable fuel dosage valve;
- with constant injector flow areas and adjustable fuel differential pressure.

Usually, the fuel pumps are integrated in the jet engine's control system; more precisely: the fuel pump is spinned by the engine's shaft (obviously, through a gear box), so the pump speed is proportional (sometimes equal) to the engine's speed, which is the engine's most frequently controlled parameter. So, the other pump control parameter (the plate angle or the discharge orifice width) must be commanded by the engine's speed controller.

Most of nowadays used aircraft jet engine controllers have as controlled parameter the engine's speed, using the fuel injection as control parameter, while the gases temperature is only a limited parameter; temperature limitation is realized through the same control parameter – the injection fuel flow rate (Moir & Seabridge, 2008; Jaw & Matingly, 2009). Consequently, a commanded fuel flow rate decrease, in order to cancel a temperature override, induces also a speed decrease.

3. Fuel injection controller with constant pressure chamber

A very simple but efficient fuel injection control constructive solution includes a fuel pump with constant pressure chamber in a control scheme for the engine's speed or exhaust gases

temperature. As far as the most important aircraft jet engine performance is the thrust level and engine's speed value is the most effective mode to estimate it, engine speed control becomes a priority.

Figure 3 presents a hydro-mechanical fuel injection control system, based on a fuel pump with plungers and constant pressure chamber.
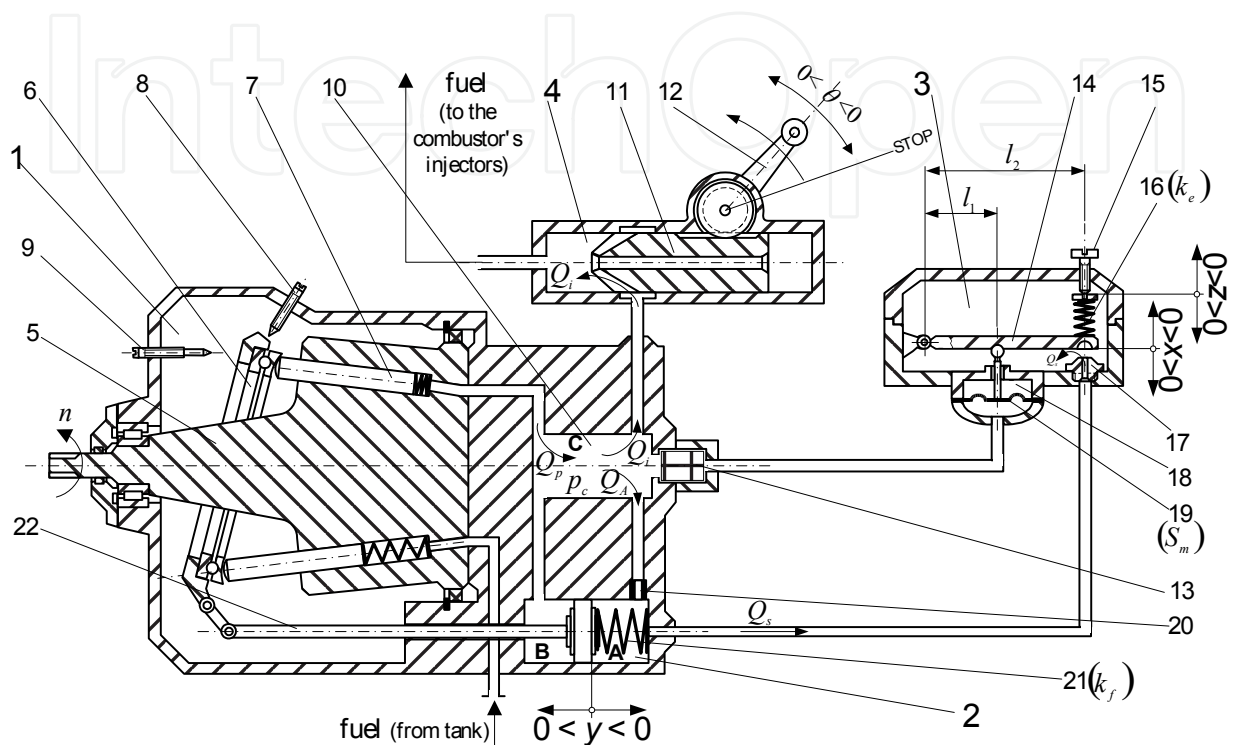

Fig. 3. Fuel injection controller with constant pressure chamber

3.1 System presentation

This type of fuel injection controller assures the requested fuel flow rate adjusting the dosage valve effective area, while the fuel pressure before it is kept constant.

Main parts of the system are: 1-fuel pump with plungers; 2-pump's actuator; 3-pressure sensor with nozzle-flap system; 4-dosage valve (dosing element). The fuel pump delivers a Q_p fuel flow rate, at a p_c pressure in a pressure chamber 10, which supplies the injector ramp through a dosage valve. This dosage valve slide 11 operates proportionally to the throttle's displacement, being moved by the lever 12. The pump is connected to the engine shaft, so its speed is n, or proportional to it. Pump 6 plate's angle is established by the actuator's rod 22-displacement y, given by the balance of the pressures in the actuator's chambers (A and B) and the 21 spring's elastic force. The pressure p_A in chamber A is given by the balance between the fuel flow rates through the drossel 20 and the nozzle 17 (covered by the semi-spherical flap, attached to the sensor's lever 14). The balance between two mechanical moments establishes the sensor lever's displacement x: the one given by the elastic force of the spring 16 (due to its z pre-compression) and the one given by the elastic force of the membrane 19 (displaced by the pressure in chamber, between the membrane and the fluid oscillations buffer 13).

The system operates by keeping a constant pressure in chamber 10, equal to the preset value (proportional to the spring 16 pre-compression, set by the adjuster bolt 15). The engine's necessary fuel flow rate Q_i and, consequently, the engine's speed n, are controlled by the co-relation between the p_c pressure's value and the dosage valve's variable slot (proportional to the lever's angular displacement θ).

An operational block diagram of the control system is presented in figure 4.
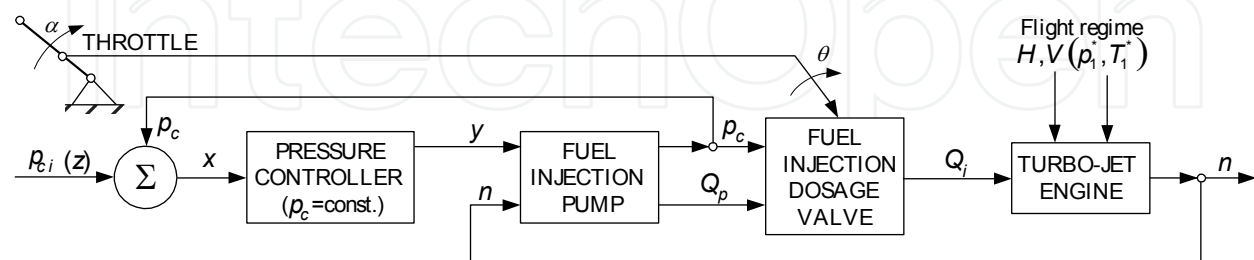

Fig. 4. Constant pressure chamber controller's operational block diagram

3.2 System mathematical model

The mathematical model consists of the motion equations for each sub-system, as follows:

a. fuel pump flow rate equation

$$Q_p = Q_p(n, y) \, , \tag{5}$$

b. constant pressure chamber equation

$$Q_i = Q_p - Q_A \, , \tag{6}$$

c. fuel pump actuator equations

$$Q_A = \mu_{dA} \frac{\pi d_A^2}{4} \sqrt{\frac{2}{\rho}} \sqrt{p_c - p_A} \, , \tag{7}$$

$$Q_A - Q_s = \beta V_{A0} \frac{dp_A}{dt} + S_A \frac{d}{dt}(y_s + y) \, , \tag{8}$$

$$m \frac{d^2 y}{dt^2} + \xi \frac{dy}{dt} + k_f (y_s + y) = S_B p_c - S_A p_A \, , \tag{9}$$

d. pressure sensor equations

$$Q_s = -\mu_n \pi d_n \sqrt{\frac{2}{\rho}} (z + x) \sqrt{p_A - p_0} \, , \tag{10}$$

$$l_1 S_m p_c + l_2 \frac{\pi d_n^2}{4} p_A = l_2 k_e (z + x) \, , \tag{11}$$

e. dosing valve equation

$$Q_i = \mu_i b_1 \frac{\theta_s + \theta}{\pi} \sqrt{\frac{2}{\rho}} \sqrt{p_c - p_{CA}} \, , \tag{12}$$

f.   jet engine's equation (considering its speed n as controlled parameter)

$$n = n\left(Q_i, p_1^*, T_1^*\right), \tag{13}$$

where Q_p, Q_i, Q_A, Q_s are fuel flow rates, p_c -pump's chamber's pressure, p_A - actuator's A chamber's pressure, p_{CA} -combustor's internal pressure, p_0 -low pressure's circuit's pressure, μ_{dA}, μ_n, μ_i -flow rate co-efficient, d_A, d_n -drossels' diameters, S_A, S_B -piston's surfaces, $S_A \approx S_B$, S_m -sensor's elastic membrane's surface, k_f, k_e -spring elastic constants, V_{A0} -actuator's A chamber's volume, β -fuel's compressibility co-efficient, ξ -viscous friction co-efficient, m-actuator's mobile ensemble's mass, θ -dosing valve's lever's angular displacement (which is proportional to the throttle's displacement), x-sensor's lever's displacement, z-sensor's spring preset, y-actuator's rod's displacement, p_1^*, T_1^* -engine's inlet's parameters (total pressure and total temperature).

It's obviously, the above-presented equations are non-linear and, in order to use them for system's studying, one has to transform them into linear equations.

Assuming the small-disturbances hypothesis, one can obtain a linear form of the model; so, assuming that each X parameter can be expressed as

$$X = X_0 + \frac{\Delta X}{1!} + \frac{(\Delta X)^2}{2!} + \dots + \frac{(\Delta X)^n}{n!} \, , \tag{14}$$

(where X_0 is the steady state regime's X-value and ΔX -deviation or static error) and neglecting the terms which contains $(\Delta X)^r, r \geq 2$, applying the finite differences method, one obtains a new form of the equation system, particularly in the neighborhood of a steady state operating regime (method described in Lungu, 2000, Stoenciu, 1986), as follows:

$$\Delta Q_A = k_A \left(\Delta p_c - \Delta p_A\right), \tag{15}$$

$$\Delta Q_i = k_{i\theta} \Delta\theta + k_{ic} \Delta p_c, \tag{16}$$

$$\Delta Q_s = k_{SA} \Delta p_A - k_s \Delta x - k_s \Delta z, \tag{17}$$

$$\Delta Q_i = \Delta Q_p - \Delta Q_A, \tag{18}$$

$$\Delta Q_A - \Delta Q_s = \beta V_{A0} \frac{\mathrm{d}}{\mathrm{d}t} \Delta p_A + S_A \frac{\mathrm{d}}{\mathrm{d}t} \Delta y, \tag{19}$$

$$k_e\left(\Delta x + \Delta z\right) = \frac{l_1}{l_2} S_m \Delta p_c, \tag{20}$$

$$\frac{k_f}{S_A}\left(\frac{m}{k_e}\frac{\mathrm{d}^2}{\mathrm{d}t^2}\Delta y + \frac{\xi}{k_e}\frac{\mathrm{d}}{\mathrm{d}t}\Delta y + 1\right) = \Delta p_c - \Delta p_A, \tag{21}$$

where the above used annotations are

$$k_A = \mu_{dA} \frac{\pi \sqrt{2} d_A^2}{8 \sqrt{\rho(p_{c0} - p_{A0})}}, k_{i\theta} = \frac{\mu_i b_1 \sqrt{2\rho p_{c0}}}{\pi \rho}, k_{SA} = \frac{\mu_n \pi d_n (x_0 + z_0) \sqrt{2\rho p_{A0}}}{2\rho p_{A0}},$$

$$k_{ic} = \frac{\mu_i b_1 (\theta_s + \theta_0) \sqrt{2\rho p_{c0}}}{2\pi\rho p_{c0}}, k_s = -\frac{\mu_n \pi d_n \sqrt{2\rho p_{A0}}}{\rho} . \tag{22}$$

Using, also, the generic annotation $\overline{X} = \frac{\Delta X}{X_0}$, the above-determined mathematical model can be transformed in a non-dimensional one. After applying the Laplace transformer, one obtains the non-dimensional linearised mathematical model, as follows

$$k_{PA}(\tau_A s + 1)\overline{p_A} + \tau_y s \overline{y} + k_{cx} \overline{x} + k_{cz} \overline{z} = \overline{p_c}, \tag{23}$$

$$k_{cx} \overline{x} + k_{cz} \overline{z} = k_{zxc} \overline{p_c}, \tag{24}$$

$$k_{Ay}(T_y^2 s^2 + 2\omega_0 T_y s + 1)\overline{y} = k_{AC} \overline{p_c} - \overline{p_A}, \tag{25}$$

$$k_{\theta} \overline{\theta} + k_{pc} \overline{p_c} - k_{py} \overline{y} = \overline{p_A}, \tag{26}$$

$$k_{cQ} \overline{p_c} - k_{\theta Q} \overline{\theta} = \overline{Q_i}. \tag{27}$$

For the complete control system determination, the fuel pump equation (for Q_p) and the jet engine equation for n (Stoicescu & Rotaru, 1999) must be added. One has considered that the engine is a single-jet single-spool one and its fuel pump is spinned by its shaft; therefore, the linearised non-dimensional mathematical model (equations 23÷27) should be completed by

$$\overline{Q_p} = k_{pn} \overline{n} + k_{py} \overline{y}, \tag{28}$$

$$(\tau_M s + 1)\overline{n} = k_c \overline{Q_i} + k_{HV} \overline{p_1^*}. \tag{29}$$

For the (23)÷(29) equation system the used co-efficient expressions are

$$k_{AC} = \frac{p_{c0}}{p_{A0}}, k_{PA} = \frac{(k_A + k_{SA})}{k_A k_{AC}}, k_{cx} = \frac{k_s x_0}{p_{c0}}, k_{cz} = \frac{k_s z_0}{p_{c0}}, \tau_A = \frac{\beta V_{A0}}{k_A + k_{SA}}, \tau_y = \frac{S_A y_0}{k_A p_{c0}}, k_{Ay} = \frac{k_e y_0}{S_A p_{c0}},$$

$$T_y = \sqrt{\frac{m}{k_e}}, \omega_0 = \frac{\xi}{2 T_y k_e}, k_{zxc} = \frac{k_s S_m p_{c0}}{k_e} \frac{l_1}{l_2}, k_{\theta} = \frac{k_{i\theta} \theta_0}{k_A p_{A0}},$$

$$k_{pc} = \frac{(k_A + k_{ic})}{k_A k_{AC}}, k_{Qp} = \frac{Q_{p0}}{k_A p_{A0}}, k_{\theta Q} = \frac{k_{i\theta} \theta_0}{Q_{i0}}, k_{cQ} = \frac{k_{ic} p_{c0}}{Q_{i0}} = k_c . \tag{30}$$

Based on some practical observation, a few supplementary hypotheses could be involved (Abraham, 1986). Thus, the fuel is a non-compressible fluid, so $\beta = 0$; the inertial effects are very small, as well as the viscous friction, so the terms containing m and ξ are becoming null. The fuel flow rate through the actuator Q_A is very small, comparative to the combustor's fuel flow rate Q_i, so $Q_p \approx Q_i$. Consequently, the new, simplified, mathematical model equations are:

- for the pressure sensor:

$$\overline{x} = k_l \, \overline{p_c} + k_z \overline{z} \, , \tag{31}$$

where

$$k_l = \frac{p_{c0}}{x_0}\left(\frac{\partial x}{\partial p_c}\right)_0 = \frac{p_{c0}}{x_0}\frac{l_1}{l_2}\frac{S_m}{k_e}, \, k_z = \frac{z_0}{x_0}\left(\frac{\partial x}{\partial z}\right)_0 \, , \tag{32}$$

or, considering that the imposed, preset value of p_c is $\overline{p_{ci}} = \frac{k_z}{k_l}\overline{z} = \frac{z_0}{p_{c0}}\left(\frac{\partial p_c}{\partial z}\right)_0$, one obtains

$$\overline{x} = -k_l\left(\overline{p_{ci}} - \overline{p_c}\right); \tag{33}$$

- for the actuator:

$$\left(\tau_y \mathrm{s} + 1\right)\overline{y} = -k_x\overline{x} \, , \tag{34}$$

where

$$\tau_y = \frac{S_A}{\left(\dfrac{\partial Q_s}{\partial y}\right)_0 - \left(\dfrac{\partial Q_A}{\partial y}\right)_0} = \frac{4S_A\sqrt{k_f y_0\left(p_{c0} - k_f y_0\right)}}{k_f\pi\left(2\mu_n d_n x_0 - \mu_{dA}d_A^2\right)}, \, p_{A0} = p_{c0} - k_f y_0 \, ,$$

$$k_x = \frac{\dfrac{y_0}{x_0}\left(\dfrac{\partial Q_s}{\partial x}\right)_0}{\left(\dfrac{\partial Q_s}{\partial y}\right)_0 - \left(\dfrac{\partial Q_A}{\partial y}\right)_0} = \frac{y_0}{x_0}\frac{4\mu_n d_n p_{A0}\sqrt{k_f y_0}}{2\mu_n d_n x_0 - \mu_{dA}d_A^2} \, . \tag{35}$$

Simplified mathematical model's new form becomes

$$\left(\tau_M \mathrm{s} + 1\right)\overline{n} = k_c\overline{Q_i} + k_{HV}\,\overline{p_1^*} \, , \tag{36}$$

$$\overline{Q_i} \equiv \overline{Q_p} = k_{pn}\overline{n} + k_{py}\overline{y} \, , \tag{37}$$

$$\overline{x} = -k_l\left(\overline{p_{ci}} - \overline{p_c}\right); \tag{38}$$

$$\left(\tau_y \mathrm{s}+1\right)\overline{y}=-k_x\overline{x} \, , \tag{39}$$

$$\overline{p_c}=\frac{1}{k_p}\overline{Q_i}-\frac{k_\theta}{k_p}\overline{\theta} \, . \tag{40}$$

One can observe that the system operates by assuring the constant value of p_c, the injection fuel flow rate being controlled through the dosage valve positioning, which means directly by the throttle. So, the system's relevant output is the p_c-pressure in chambers 10.

For a constant flight regime, altitude and airspeed ($H=\mathrm{const.}, V=\mathrm{const.}$), which mean that the air pressure and temperature before the engine's compressor are constant $\left(p_1^*=\mathrm{const.}, T_1^*=\mathrm{const.}\right)$, the term in equation (36) containing $\overline{p_1^*}$ becomes null.

3.3 System transfer function

Based on the above-presented mathematical model, one has built the block diagram with transfer functions (see figure 5) and one also has obtained a simplified expression:

$$\left\{\tau_y\tau_M\mathrm{s}^2+\left[\left(1-k_c k_{pn}\right)\tau_y+\left(1+\frac{k_r k_{py}}{k_p}\right)\tau_M\right]\mathrm{s}+\left(1-k_c k_{pn}\right)+\frac{k_r k_{py}}{k_p}\right\}\overline{p_c}=$$

$$-\frac{k_\theta}{k_p}\left(\tau_y\mathrm{s}+1\right)\left(\tau_M\mathrm{s}+1-k_c k_{pn}\right)\overline{\theta}+\frac{k_{py}k_r}{k_p}\left(\tau_M\mathrm{s}+1\right)\overline{p_{ci}} \, , \tag{41}$$
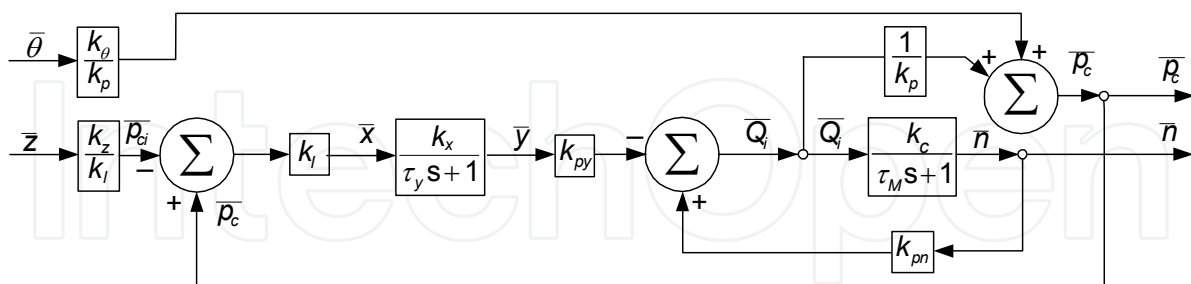
where $k_r=k_x k_l$.

Fig. 5. System's block diagram with transfer functions

So, one can define two transfer functions:
a. with respect to the dosage valve's lever angular displacement $H_\theta(\mathrm{s})$;
b. with respect to the preset reference pressure p_{ci}, or to the sensor's spring's pre-compression z, $H_z(\mathrm{s})$.

While θ angle is permanently variable during the engine's operation, the reference pressure's value is established during the engine's tests, when its setup is made and

remains the same until its next repair or overhaul operation, so $\bar{z} = \overline{p_{ci}} = 0$ and the transfer function $H_z(\text{s})$ definition has no sense. Consequently, the only system's transfer function remains

$$H_\theta(\text{s}) = \frac{-\dfrac{k_\theta}{k_p}\left(\tau_y\text{s}+1\right)\left(\tau_M\text{s}+1-k_ck_{pn}\right)}{\tau_y\tau_M\text{s}^2 + \left[\left(1-k_ck_{pn}\right)\tau_y + \left(1+\dfrac{k_rk_{py}}{k_p}\right)\tau_M\right]\text{s} + 1 - k_ck_{pn} + \dfrac{k_rk_{py}}{k_p}}, \tag{42}$$

which characteristic polynomial's degree is 2.

3.4 System stability

One can perform a stability study, using the Routh-Hurwitz criteria, which are easier to apply because of the characteristic polynomial's form. So, the stability conditions are

$$\tau_y\tau_M > 0, \tag{43}$$

$$\left(1-k_ck_{pn}\right)\tau_y + \left(1+\frac{k_rk_{py}}{k_p}\right)\tau_M > 0, \tag{44}$$

$$1 - k_ck_{pn} + \frac{k_rk_{py}}{k_p} > 0. \tag{45}$$

The first condition (43) is obviously, always realized, because both τ_y and τ_M are strictly positive quantities, being time constant of the actuator, respectively of the engine.

The (40) and (41) conditions must be discussed.

The factor $1-k_ck_{pn}$ is very important, because its value is the one who gives information about the stability of the connection between the fuel pump and the engine's shaft (Stoicescu&Rotaru, 1999). There are two situation involving it:

a. $k_ck_{pn} < 1$, when the connection between the fuel pump and the engine shaft is a stable controlled object;

b. $k_ck_{pn} \geq 1$, when the connection fuel pump - engine shaft is an unstable object and it is compulsory to be assisted by a controller.

If $k_ck_{pn} < 1$, the factor $1-k_ck_{pn}$ is strictly positive, so $\left(1-k_ck_{pn}\right)\tau_y > 0$. According to their definition formulas (see annotations (35) and (30)), k_r, k_p, k_{py} are positive, so $\dfrac{k_rk_{py}}{k_p} > 0$ and $\left(1+\dfrac{k_rk_{py}}{k_p}\right)\tau_M > 0$, which means that both other stability requests, (44) and (45), are accomplished, that means that the system is a stable one for any situation.

If $k_c k_{pn} \geq 1$, the factor $1 - k_c k_{pn}$ becomes a negative one. The inequality (44) leads to

$$\tau_M < \frac{\left(k_c k_{pn} - 1\right)}{\left(1 + \dfrac{k_r k_{py}}{k_p}\right)} \tau_y \text{ , or } \tau_y < \frac{\left(1 + \dfrac{k_r k_{py}}{k_p}\right)}{\left(k_c k_{pn} - 1\right)} \tau_M \text{ ,} \tag{46}$$

which offers a criterion for the time constant choice and establishes the boundaries of the stability area (see figure 6.a).

Meanwhile, from the inequality (45) one can obtain a condition for the sensor's elastic membrane surface area's choice, with respect to the drossels' geometry (d_A, d_n) and quality (μ_n, μ_A), springs' elastic constants (k_e, k_f), sensor's lever arms (l_1, l_2) and other stability co-efficient (k_c, k_{pn}, k_{py})

$$S_m > \frac{k_e}{k_f} \frac{l_2}{l_1} \frac{k_c k_{pn} - 1}{k_{py}} \frac{\left(2\mu_n d_n x_0 - \mu_{dA} d_A^2\right)\sqrt{2\rho k_f y_0}}{4\mu d_n p_{A0}} \text{ .} \tag{47}$$

Another observation can be made, concerning the character of the stability, periodic or non-periodic. If the characteristic equation's discriminant is positive (real roots), than the system's stability is non-periodic type, otherwise (complex roots) the system's stability is periodic type. Consequently, the non-periodic stability condition is

$$\left[\left(1 - k_c k_{pn}\right)\tau_y + \left(1 + \frac{k_r k_{py}}{k_p}\right)\tau_M\right]^2 - 4\tau_y \tau_M + \frac{k_r k_{py}}{k_p} > 0 \text{ ,} \tag{48}$$

which leads to the inequalities

$$\frac{\tau_y}{\tau_M} < \frac{k_p\left(k_c k_{pn} - 1\right)\left[k_r k_{py} - k_p - \sqrt{2\left(k_p^2 + k_r^2 k_{py}^2\right)}\right]}{k_p^2 + k_r k_{py}\left(2k_p + k_r k_{py}\right)} \text{ ,} \tag{49}$$

$$\frac{\tau_y}{\tau_M} > \frac{k_p\left(k_c k_{pn} - 1\right)\left(k_r k_{py} - k_p + \sqrt{2\left(k_p^2 + k_r^2 k_{py}^2\right)}\right)}{k_p^2 + k_r k_{py}\left(2k_p + k_r k_{py}\right)} \text{ ,} \tag{50}$$

representing two semi-planes, which boundaries are two lines, as figure 6.b shows; the area between the lines is the periodic stability domain, respectively the areas outside are the non-periodic stability domains.

Obviously, both time constants must be positive, so the domains are relevant only for the positives sides of τ_y and τ_M axis.

Both figures (6.a and 6.b) are showing the domains for the pump actuator time constant choice or design, with respect to the jet engine's time constant.

The studied system can be characterized as a 2nd order controlled object. For its stability, the most important parameters are engine's and actuator's time constants; a combination of a small τ_y and a big τ_M, as well as vice-versa (until the stability conditions are accomplished), assures the non periodic stability, but comparable values can move the stability into the periodic domain; a very small τ_y and a very big τ_M are leading, for sure, to instability.
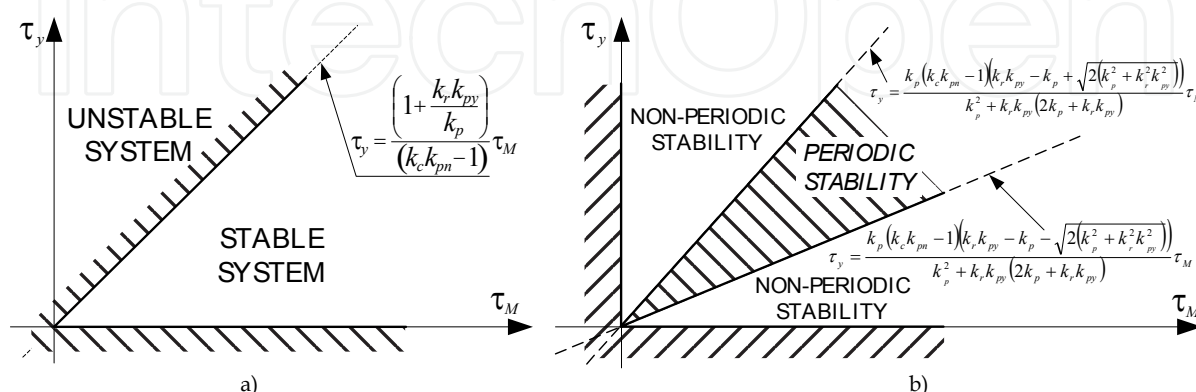

Fig. 6. System's stability domains

3.4 System quality

As the transfer function form shows, the system is static one, being affected by static error.
One has studied/simulated a controller serving on an engine RD-9 type, from the point of view of the step response, which means the system's behavior for step input of the dosage valve's lever's angle θ.

System's time responses, for the fuel injection pressure p_c and for the engine's speed n are

$$\overline{p_c}(t) = \frac{-k_\theta}{k_p}\left(1 - \frac{1}{1 + \dfrac{k_r k_{py}}{1 - k_c k_{pn}}}\right)\overline{\theta}(t),\tag{51}$$

$$\overline{n}(t) = \frac{k_\theta k_c k_r}{k_p\left(1 - k_c k_{pn}\right) + k_r k_{py}}\overline{\theta}(t),\tag{52}$$

as shown in figure 7.a). One can observe that the pressure p_c has an initial step decreasing, $p_c(0) = -\dfrac{k_\theta}{k_p}$, then an asymptotic increasing; meanwhile, the engine's speed is continuous asymptotic increasing.

One has also performed a simulation for a hypothetic engine, which has such a co-efficient combination that $k_c k_{pn} \geq 1$; even in this case the system is a stable one, but its stability happens to be periodic, as figure 7.b) shows. One can observe that both the pressure and the speed have small overrides (around 2.5% for n and 1.2% for p_c) during their stabilization.

The chosen RD-9 controller assures both stability and asymptotic non-periodic behavior for the engine's speed, but its using for another engine can produce some unexpected effects.
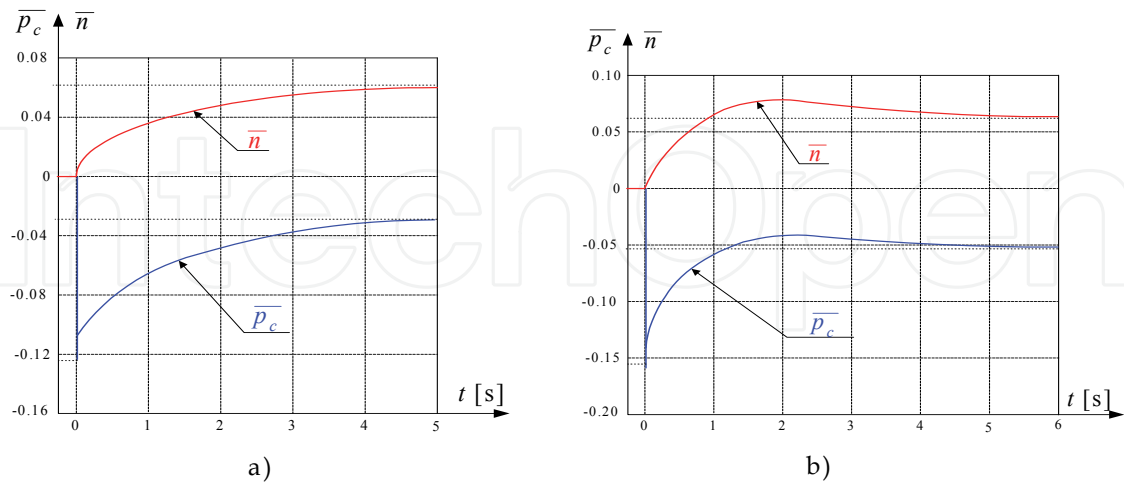

Fig. 7. System's quality (system time response for θ-step input)

4. Fuel injection controller with constant differential pressure

Another fuel injection control system is the one in figure 8, which assures a constant value of the dosage valve's differential pressure $p_c - p_i$, the fuel flow rate amount Q_i being determined by the dosage valve's opening.

As figure 8 shows, a rotation speed control system consists of four main parts: I-fuel pump with plungers (4) and mobile plate (5); II-pump's actuator with spring (22), piston (23) and rod (6); III-differential pressure sensor with slide valve (17), preset bolt (20) and spring (18); IV-dosage valve, with its slide valve (11), connected to the engine's throttle through the rocking lever (13).
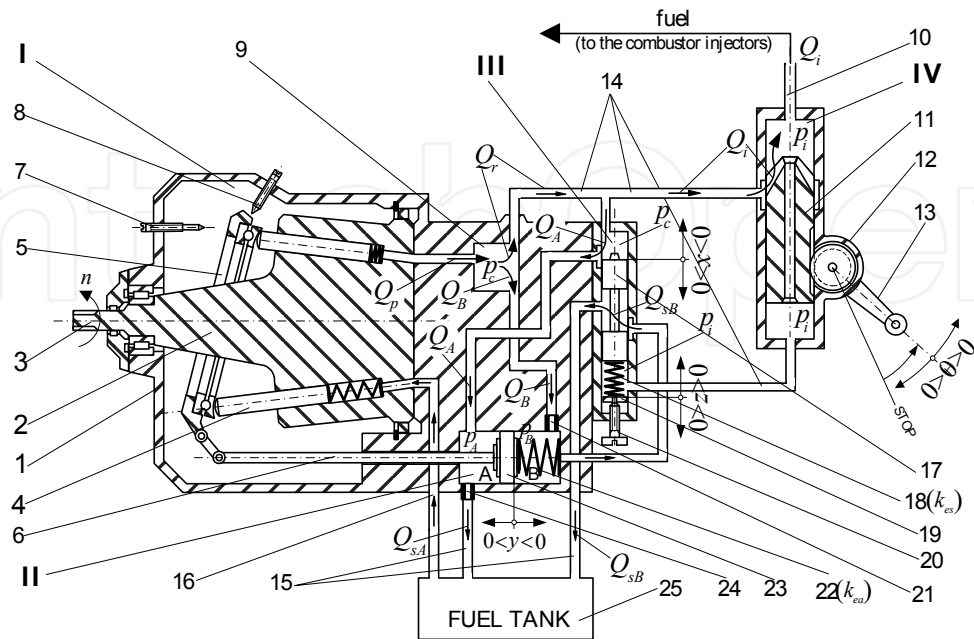

Fig. 8. Fuel injection controller with constant differential pressure $p_r = p_c - p_i$

The system operates by keeping a constant difference of pressure, between the pump's pressure chamber (9) and the injectors' pipe (10), equal to the preset value (proportional to the spring (18) pre-compression, set by the adjuster bolt (20)). The engine's necessary fuel flow rate Q_i and, consequently, the engine's speed n, are controlled by the co-relation between the $p_r = p_c - p_i$ differential pressure's amount and the dosage valve's variable slot opening (proportional to the (13) rocking lever's angular displacement θ).

4.1 Mathematical model and transfer function

The non-linear mathematical model consists of the motion equations for each above described sub-system In order to bring it to an operable form, assuming the small perturbations hypothesis, one has to apply the finite difference method, then to bring it to a non-dimensional form and, finally, to apply the Laplace transformer (as described in 3.2). Assuming, also, that the fuel is a non-compressible fluid, the inertial effects are very small, as well as the viscous friction, the terms containing m, β and ξ are becoming null. Consequently, the simplified mathematical model form shows as follows

$$\left(\tau_p s + 1\right)\left(\overline{p_B} - \overline{p_A}\right) = -k_{px}\overline{x} ,\tag{53}$$

$$\overline{p_B} - \overline{p_A} = k_{AB}\overline{y} ,\tag{54}$$

$$\overline{x} = \frac{1}{k_{pic}}\left(\overline{p_c} - \overline{p_i}\right) - \frac{k_{iz}}{k_{pic}}\overline{z} ,\tag{55}$$

$$\overline{p_c} - \overline{p_i} = \frac{1}{k_{Qp}}\left(\overline{Q_p} - k_\theta\overline{\theta} - k_{Qx}\overline{x}\right) ,\tag{56}$$

$$\overline{Q_i} = \overline{Q_p} - k_\theta\overline{\theta} ,\tag{57}$$

$$\overline{Q_p} = k_{pn}\overline{n} + k_{py}\overline{y} .\tag{58}$$

The model should be completed by the jet engine as controlled object equation

$$\left(\tau_M s + 1\right)\overline{n} = k_c\overline{Q_i} + k_{HV}\overline{p_1^*} ,\tag{59}$$

where, for a constant flight regime, the term $k_{HV}\overline{p_1^*}$ becomes null.

The equations (53) to (59), after eliminating the intermediate arguments $\overline{p_A}, \overline{p_B}, \overline{p_c}, \overline{p_i}, \overline{Q_i}, \overline{Q_p}, \overline{y}, \overline{x}$, are leading to a unique equation:

$$\left[\left(k_{pic} + k_{Qx}\right)\frac{k_{AB}}{k_{px}}\left(\tau_p s + 1\right)\frac{\tau_M s + \left(1 - k_c k_{pn}\right)}{k_c k_{py}} - \frac{\tau_M s + 1}{k_c}\right]\overline{n} = k_{iz}\overline{z} + \left(k_{pic} + k_{Qx}\right)\frac{k_{AB}k_\theta}{k_{px}k_{py}}\left(\tau_p s + 1\right)\overline{\theta} .\tag{60}$$

System's transfer function is $H_\theta(s)$, with respect to the dosage valve's rocking lever's position θ. A transfer function with respect to the setting z, $H_z(s)$, is not relevant, because the setting and adjustments are made during the pre-operational ground tests, not during the engine's current operation.

So, the main and the most important transfer function has the form below

$$H_\theta(s) = \frac{f_1 s + f_0}{g_2 s^2 + g_1 s + g_0} , \tag{61}$$

where the involved co-efficient are $\quad f_1 = k_c k_\theta \tau_p , \; f_0 = k_c k_\theta , \; g_2 = \tau_p \tau_M ,$

$$g_1 = \tau_p\left(1 - k_c k_{pn}\right) + \tau_M\left[1 - \frac{k_{px} k_{py}}{k_{AB}\left(k_{pic} + k_{Qx}\right)}\right], \quad g_0 = \left(1 - k_c k_{pn}\right) - \frac{k_{px} k_{py}}{k_{AB}\left(k_{pic} + k_{Qx}\right)} . \tag{62}$$

4.2 System quality

As the transfer function shows, the system is a static-one, being affected by static error.

One has studied/simulated a controller serving on a single spool jet engine (VK-1 type), from the point of view of the step response, which means the system's dynamic behavior for a step input of the dosage valve's lever's angle θ.

According to figure 9.a), for a step input of the throttle's position α, as well as of the lever's angle θ, the differential pressure $p_r = p_c - p_i$ has an initial rapid lowering, because of the initial dosage valve's step opening, which leads to a diminution of the fuel's pressure p_c in the pump's chamber; meanwhile, the fuel flow rate through the dosage valve grows. The differential pressure's recovery is non-periodic, as the curve in figure 9.a) shows.

Theoretically, the differential pressure re-establishing must be made to the same value as before the step input, but the system is a static-one and it's affected by a static error, so the new value is, in this case, higher than the initial one, the error being 4.2%. The engine's speed has a different dynamic behavior, depending on the $k_c k_{pn}$ particular value.
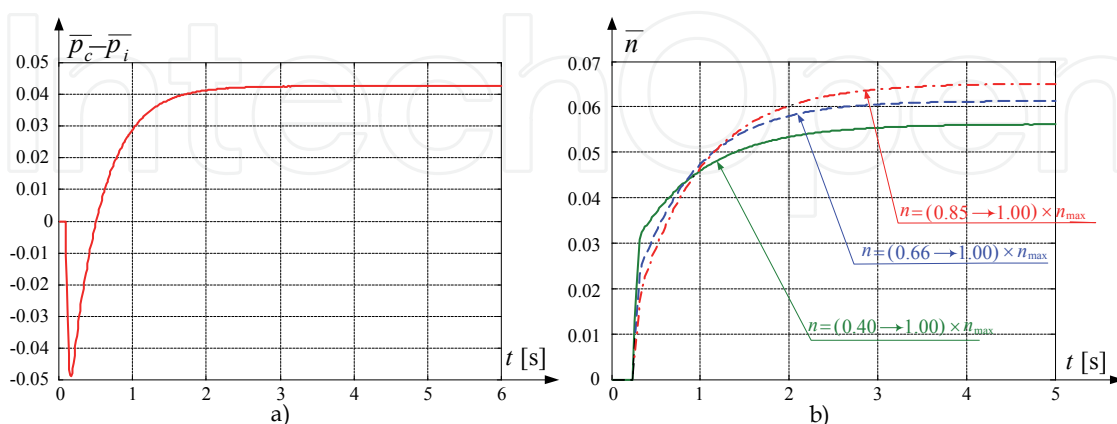

Fig. 9. System's quality (system time response for θ-step input)

One has performed simulations for a VK-1-type single-spool jet engine, studying three of its operating regimes: a) full acceleration (from idle to maximum, that means from

$0.4 \times n_{\max}$ to $n_{\max}$); b) intermediate acceleration (from $0.65 \times n_{\max}$ to $n_{\max}$); c) cruise acceleration (from $0.85 \times n_{\max}$ to $n_{\max}$).

If $k_c k_{pn} < 1$, so the engine is a stable system, the dynamic behavior of its rotation speed n is shown in figure 9.b). One can observe that, for any studied regime, the speed n, after an initial rapid growth, is an asymptotic stable parameter, but with static error. The initial growing is maxim for the full acceleration and minimum for the cruise acceleration, but the static error behaves itself in opposite sense, being minimum for the full acceleration.

5. Fuel injection controller with commanded differential pressure

Unlike the precedent controller, where the differential pressure was kept constant and the fuel flow rate was given by the dosage valve opening, this kind of controller has a constant injection orifice and the fuel flow rate variation is given by the commanded differential pressure value variation. Such a controller is presented in figure 10, completed by two correctors (a barometric corrector VII and an air flow rate corrector VIII, see 5.3).

The basic controller has four main parts (the pressure transducer I, the actuator II, the actuator's feed-back III and the fuel injector IV); it operates together with the fuel pump V, the fuel tank VI and, obviously, with the turbo-jet engine.
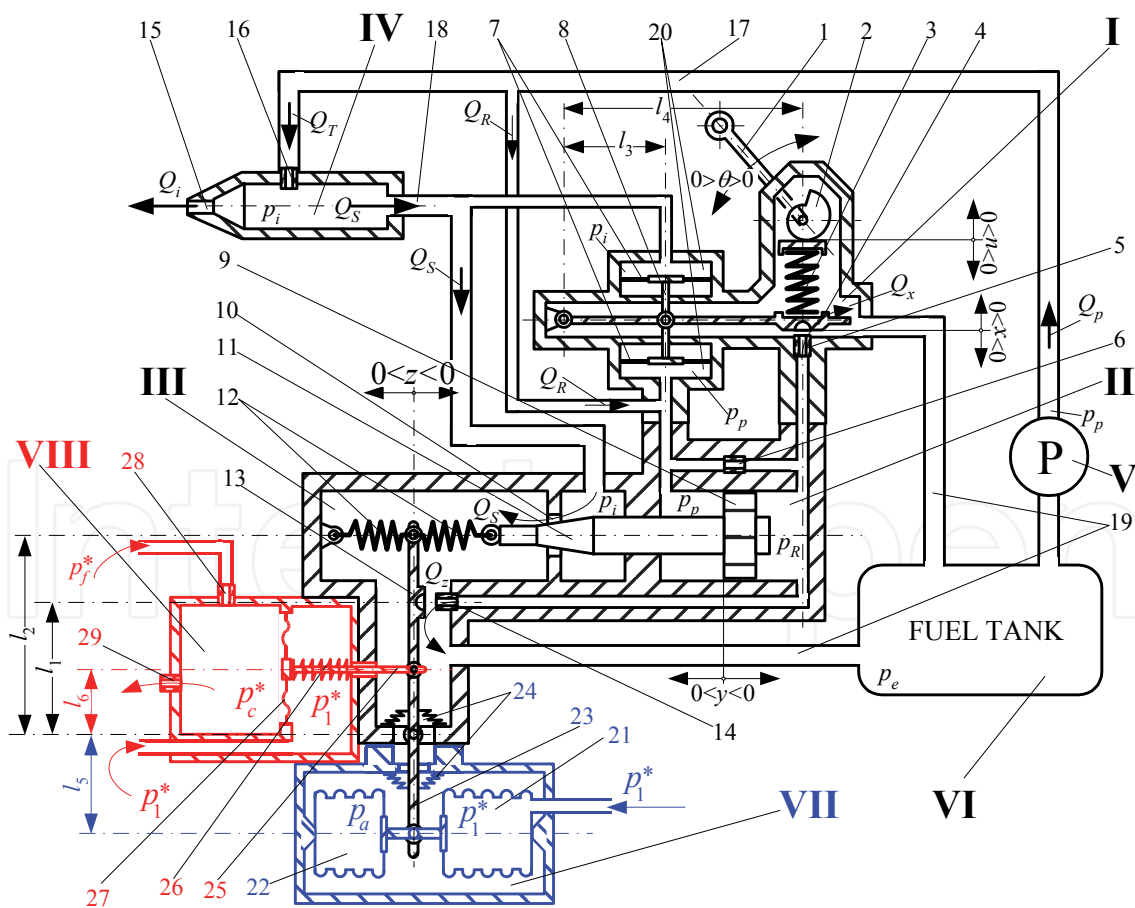

Fig. 10. Fuel injection controller with commanded differential pressure $p_r = p_c - p_i$ (basic controller), with barometric corrector and air flow rate corrector

Controller's duty is to assure, in the injector's chamber, the appropriate p_i value, enough to assure the desired value of the engine's speed, imposed by the throttle's positioning, which means to co-relate the pressure difference $p_p - p_i$ to the throttle's position (given by the 1 lever's θ -angle).

The fuel flow rate Q_i, injected into the engine's combustor, depends on the injector's diameter (drossel no. 15) and on the fuel pressure in its chamber p_i. The difference $p_p - p_i$, as well as p_i, are controlled by the level of the discharged fuel flow Q_S through the calibrated orifice 10, which diameter is given by the profiled needle 11 position; the profiled needle is part of the actuator's rod, positioned by the actuator's piston 9 displacement.

The actuator has also a distributor with feedback link (the flap 13 with its nozzle or drossel 14, as well as the springs 12), in order to limit the profiled needle's displacement speed.

Controller's transducer has two pressure chambers 20 with elastic membranes 7, for each measured pressure p_p and p_i; the inter-membrane rod is bounded to the transducer's flap 4. Transducer's role is to compare the level of the realized differential pressure $p_p - p_i$ to its necessary level (given by the 3 spring's elastic force, due to the (lever1+cam2) ensemble's rotation). So, the controller assures the necessary fuel flow rate value Q_i, with respect to the throttle's displacement, by controlling the injection pressure's level through the fuel flow rate discharging.

5.1 System mathematical model and block diagram with transfer functions

Basic controller's linear non-dimensional mathematical model can be obtained from the motion equations of each main part, using the same finite differences method described in chapter 3, paragraph 3.2, based on the same hypothesis.

The simplified mathematical model form is, as follows

$$\overline{p_R} = k_{1p}\overline{p_p} - k_{1x}\overline{x} - k_{1y}\left(\tau_y s + 1\right)\overline{y} \ , \tag{63}$$

$$\overline{p_p} = k_{2p}\overline{p_i} + k_{2R}\overline{p_R} + k_{2Q}\overline{Q_p} \ , \tag{64}$$

$$\overline{y} = k_{yR}\overline{p_R} - k_{yp}\overline{p_p} \ , \tag{65}$$

$$\overline{p_i} = k_{3p}\overline{p_p} - k_{3y}\overline{y} \ , \tag{66}$$

$$\overline{Q_i} = k_i\overline{p_i} \ , \ \overline{u} = k_{u\theta}\overline{\theta} \ , \tag{67}$$

together with the fuel pump and the engine's speed non-dimensional equations

$$\overline{Q_p} = k_{pn}\overline{n} \ , \tag{68}$$

$$\left(\tau_m s + 1\right)\overline{n} = k_c\overline{Q_i} + k_{HV}\overline{p_1^*} \ . \tag{69}$$

where the used annotations are

$$k_{PT} = \mu_d \frac{\pi d_{16}^2}{4} \frac{1}{\sqrt{2\rho\left(p_{p0} - p_{i0}\right)}} , k_{xx} = \mu_4\pi d_4\sqrt{\frac{2p_{R0}}{\rho}} , k_{Qi} = \mu_d \frac{\pi d_i^2}{4}\frac{1}{\sqrt{2\rho p_{p0}}} , k_{zz} = \mu_{11}\pi d_{11}\sqrt{\frac{2p_{R0}}{\rho}} ,$$

$$k_{RP} = \mu_7 \frac{\pi d_7^2}{4} \frac{1}{\sqrt{2\rho(p_{p0} - p_{R0})}} \, , \ k_{sy} = \mu \frac{\pi}{4}\Big[d_0^2 - d_1^2 - 4(d_1 - y_0 \tan\alpha)\tan\alpha \Big] \sqrt{\frac{2p_{i0}}{\rho}} \, ,$$

$$k_{si} = \mu \frac{\pi}{4}\Big[d_0^2 - d_1^2 - 4(d_1 - y_0 \tan\alpha)\tan\alpha \Big] \frac{1}{\sqrt{2\rho p_{i0}}} \, , \ k_{zR} = \mu_{11}\pi d_{11}(z_0 - z_s)\sqrt{\frac{1}{2\rho p_{R0}}} \, ,$$

$$k_{xR} = \mu_4 \pi d_4 (x_0 - x_s)\sqrt{\frac{1}{2\rho p_{R0}}} \, , \ k_{u\theta} = k_\theta \frac{\theta_0}{u_0} \, , \ k_{xd} = \frac{S_m l_3 p_{d0}}{k_{rs} l_4 x_0} \, , \ k_u = \frac{u_0}{x_0} \, , \ k_{dp} = \frac{p_{p0}}{p_{d0}} \, , \ k_{di} = \frac{p_{i0}}{p_{d0}} \, ,$$

$$k_{1p} = \frac{k_{RP} p_{p0}}{(k_{RP} + k_{xR} + k_{zR})p_{R0}} \, , \ \tau_y = \frac{S_R l_2}{k_{zz} l_1} \, , \ k_{1y} = \frac{k_{zz} l_1 y_0}{p_{R0} l_2} \, , \ k_{1x} = \frac{k_{xx} x_0}{(k_{RP} + k_{xR} + k_{zR})p_{R0}} \, , \ k_i = \frac{k_{Qi} p_{i0}}{Q_{i0}}$$

$$k_{2p} = \frac{k_{PT} p_{i0}}{(k_{RP} + k_{PT})p_{p0}} \, , \ k_{2R} = \frac{k_{RP} p_{R0}}{(k_{RP} + k_{PT})p_{p0}} \, , \ k_{2Q} = \frac{Q_{p0}}{(k_{RP} + k_{PT})p_{p0}} \, , \ k_{yR} = \frac{S_R p_{R0}}{(k_{r1} + k_{r2})y_0} \, ,$$

$$k_{yp} = \frac{S_P p_{p0}}{(k_{r1} + k_{r2})y_0} \, , \ k_{3p} = \frac{k_{PT} p_{p0}}{(k_{PT} + k_{si} + k_{Qi})p_{i0}} \, , \ k_{3y} = \frac{k_{sy} y_0}{(k_{PT} + k_{si} + k_{Qi})p_{i0}} \, , \ k_{pn} = \frac{n_0}{Q_{p0}}\left(\frac{\partial Q_p}{\partial n} \right)_0 . \quad (70)$$

Furthermore, if the input signal u is considered as the reference signal forming parameter, one can obtain the expression

$$\overline{x} = -k_{xd}\left(\overline{p_{d_{ref}}} - \overline{p_d} \right) , \quad (71)$$

where $\overline{p_{d_{ref}}}$ is the reference differential pressure, given by $\quad \overline{p_{d_{ref}}} = \dfrac{k_\theta k_{rs} l_4}{S_m l_3 p_{d0}}\overline{\theta} = k_{r\theta}\overline{\theta}$.

A block diagram with transfer functions, both for the basic controller and the correctors' block diagrams (colored items), is presented in figure 11.

Fig. 11. Block diagram with transfer functions

5.2 System quality

As figures 10 and 11 show, the basic controller has two inputs: a) throttle's position - or engine's operating regime - (given by θ-angle) and b) aircraft flight regime (altitude and airspeed, given by the inlet inner pressure p_1^*). So, the system should operate in case of disturbances affecting one or both of the input parameters $\left(\overline{\theta}, \overline{p_1^*}\right)$.

A study concerning the system quality was realized (using the co-efficient values for a VK-1F jet engine), by analyzing its step response (system's response for step input for one or for both above-mentioned parameters). As output, one has considered the differential pressure $\overline{p_d}$, the engine speed $\overline{n}$ (which is the most important controlled parameter for a jet engine) and the actuator's rod displacement $\overline{y}$ (same as the profiled needle).

Output parameters' behavior is presented by the graphics in figure 12; the situation in figure 12.a) has as input the engine's regime (step throttle's repositioning) for a constant flight regime; in the mean time, the situation in figure 12.b) has as input the flight regime (hypothetical step climbing or diving), for a constant engine regime (throttle constant position). System's behavior for both input parameters step input is depicted in figure 12.a).

One has also studied the system's behavior for two different engine's models: a stable-one (which has a stabile pump-engine connection, its main co-efficient being $k_c k_{pn} < 1$, situation in figure 13.a) and a non-stable-one (which has an unstable pump-engine connection and $k_c k_{pn} > 1$, see figure 13.b).
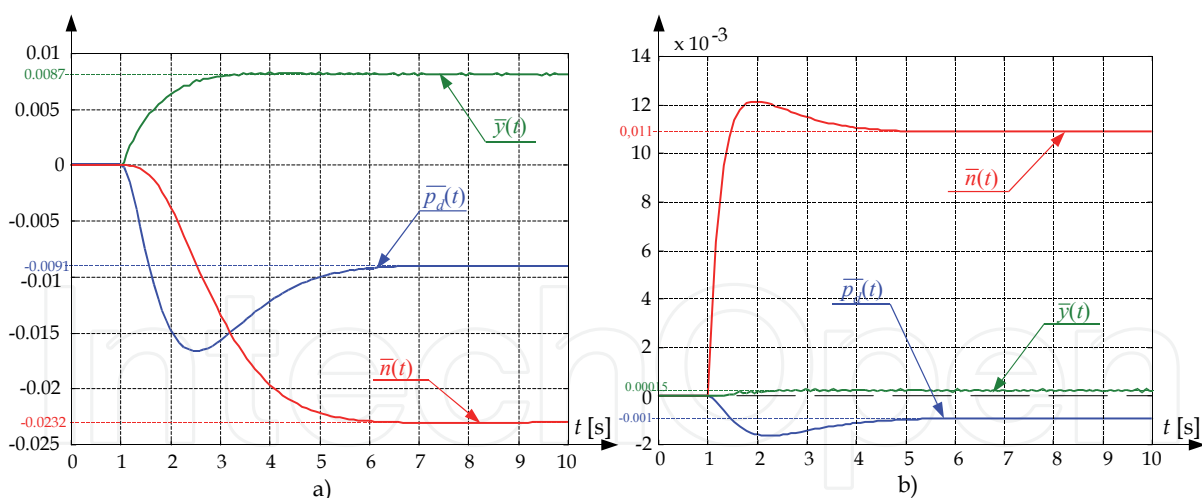
Fig. 12. Basic system step response a) step input for $\overline{\theta}$ $\left(\overline{p_1^*} = 0\right)$; b) step input for $\overline{p_1^*}$ $\left(\overline{\theta} = 0\right)$

Concerning the system's step response for throttle's step input, one can observe that all the output parameters are stables, so the system is a stable-one. All output parameters are stabilizing at their new values with static errors, so the system is a static-one. However, the static errors are acceptable, being fewer than 2.5% for each output parameter. The differential pressure and engine's speed static errors are negative, so in order to reach the engine's speed desired value, the throttle must be supplementary displaced (pushed).

For immobile throttle and step input of $\overline{p_1^*}$ (flight regime), system's behavior is similar (see figure 12.b), but the static errors' level is lower, being around 0.1% for $\overline{p_d}$ and for $\overline{y}$, but higher for $\overline{n}$ (around 1.1%, which mean ten times than the others).

When both of the input parameters have step variations, the effects are overlapping, so system's behavior is the one in figure 13.a).

System's stability is different, for different analyzed output parameters: $\overline{y}$ has a non-periodic stability, no matter the situation is, but $\overline{p_d}$ and $\overline{n}$ have initial stabilization values overriding. Meanwhile, curves in figures 12.a), 12.b) and 13.a) are showing that the engine regime has a bigger influence than the flight regime above the controller's behavior.

One also had studied a hypothetical controller using, assisting an unstable connection engine-fuel pump. One has modified k_c and k_{pn} values, in order to obtain such a combination so that $k_c k_{pn} > 1$. Curves in figure 13.b are showing a periodical stability for a controller assisting an unstable connection engine-fuel pump, so the controller has reached its limits and must be improved by constructive means, if the non-periodic stability is compulsory.
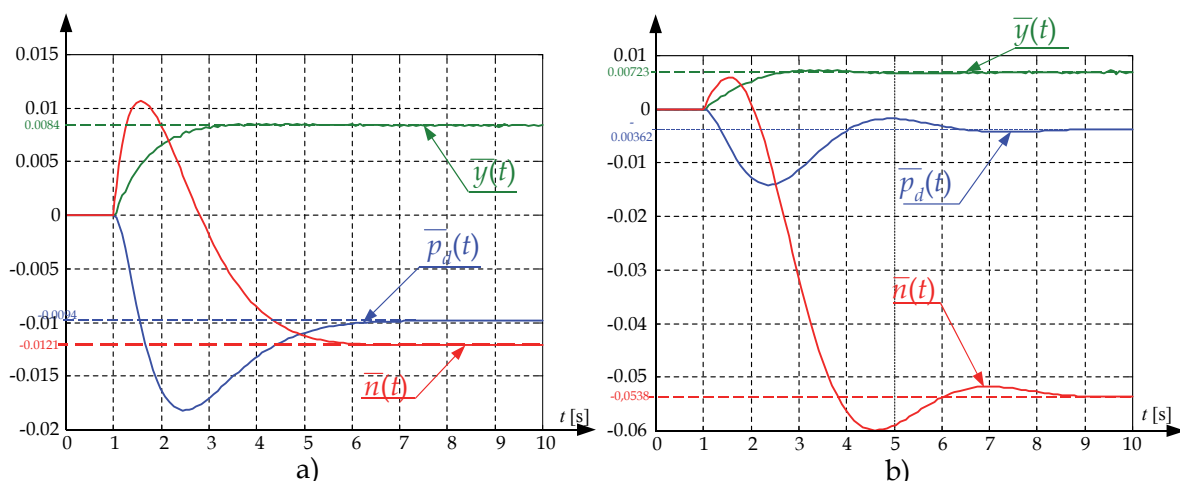
Fig. 13. Compared step response between a) stabile fuel pump-engine connection $\left(k_c k_{pn} < 1\right)$ and b) unstable fuel pump-engine connection $\left(k_c k_{pn} > 1\right)$

5.3 Fuel injection controller with barometric and air flow rate correctors
5.3.1 Correctors using principles
For most of nowadays operating controllers, designed and manufactured for modern jet engines, their behavior is satisfying, because the controlled systems become stable and their main output parameters have a non-periodic (or asymptotic) stability. However, some observations regarding their behavior with respect to the flight regime are leading to the conclusion that the more intense is the flight regime, the higher are the controllers' static errors, which finally asks a new intervention (usually from the human operator, the pilot) in order to re-establish the desired output parameters levels. The simplest solution for this issue is the flight regime correction, which means the integration in the control system of

new equipment, which should adjust the control law. These equipments are known as barometric (bar-altimetric or barostatic) correctors.

In the mean time, some unstable engines or some unstable fuel pump-engine connections, even assisted by fuel controllers, could have, as controlled system, periodic behavior, that means that their output main parameters' step responses presents some oscillations, as figure 14 shows. The immediate consequence could be that the engine, even correctly operating, could reach much earlier its lifetime ending, because of the supplementary induced mechanical fatigue efforts, combined with the thermal pulsatory efforts, due to the engine combustor temperature periodic behavior.

As fig. 14 shows, the engine speed n and the combustor temperature T_3^* (see figure 14.b), as well as the fuel differential pressure p_d and the pump discharge slide-valve displacement y (see figure 14.a) have periodic step responses and significant overrides (which means a few short time periods of overspeed and overheat for each engine full acceleration time).

The above-described situation could be the consequence of a miscorrelation between the fuel flow rate (given by the connection controller-pump) and the air flow rate (supplied by the engine's compressor), so the appropriate corrector should limit the fuel flow injection with respect to the air flow supplying.
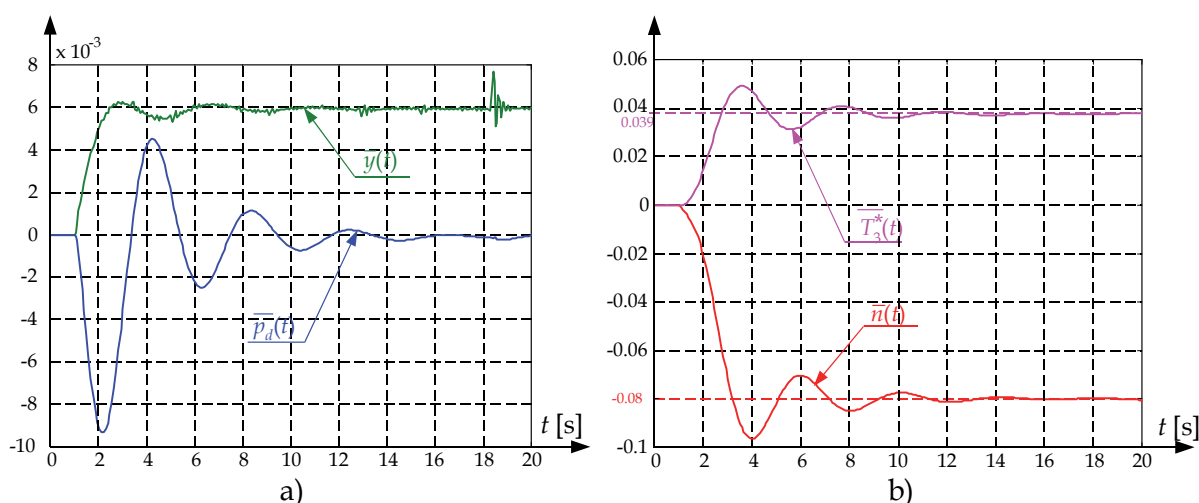
Fig. 14. Step response for an unstable fuel pump-engine connection assisted by a fuel injection pressure controller

The system depicted in figure 10 has as main control equipment a fuel injection controller (based on the differential pressure control) and it is completed by a couple of correction equipment (correctors), one for the flight regime and the other for the fuel-air flow rates correlation.

The correctors have the active parts bounded to the 13-lever (hemi-spherical lid's support of the nozzle-flap actuator's distributor). So, the 13-lever's positioning equation should be modified, according to the new pressure and forces distribution.

5.3.2 Barometric corrector

The barometric corrector (position VII in figure 10) consists of an aneroid (constant pressure) capsule and an open capsule (supplied by a p_1^* - total pressure intake), bounded by a common rod, connected to the 13-lever.

The total pressure p_1^* (air's total pressure after the inlet, in the front of the engine's compressor) is an appropriate flight regime estimator, having as definition formula

$$p_1^* = p_H \Pi\left(M_H\right)\sigma_c^* ,\tag{72}$$

where p_H is the air static pressure of the flight altitude H, σ_c^* – inlet's inner total pressure lose co-efficient (assumed as constant), M_H – air's Mach number in the front of the inlet, k – air's adiabatic exponent and $\Pi\left(M_H\right) = \left(1 + \dfrac{k-1}{2}M_H^2\right)^{\frac{k}{k-1}}$.

The new equation of the 13-lever becomes

$$S_R p_R - S_p p_p = m_s \frac{\mathrm{d}^2 y}{\mathrm{d}t^2} + \xi \frac{\mathrm{d}y}{\mathrm{d}t} + \left(k_{r1} + k_{r2}\right)y - S_H\left(p_1^* - p_a\right)\frac{l_5}{l_2} ,\tag{73}$$

where p_a is the aneroid capsule's pressure and, after the linearization and the Laplace transformer applying, its new non-dimensional form becomes

$$k_{yR}\overline{p_R} - k_{yp}\overline{p_p} - k_{yH}\overline{p_1^*} = \left(T_y^2 s^2 + 2\omega_0 T_y s + 1\right)\overline{y} \cong \overline{y} ,\tag{74}$$

and will replace the (65)-equation (see paragraph 5.2), where $k_{yH} = \dfrac{S_H p_{10}^*}{\left(k_{r1} + k_{r2}\right)y_0}\dfrac{l_5}{l_2}$.

5.3.3 Air flow-rate corrector

The air flow-rate corrector (position VIII in figure 10) consists of a pressure ratio transducer, which compares the realized pressure ratio value for a current speed engine to the preset value. The air flow-rate Q_a is proportional to the total pressure difference $p_2^* - p_1^*$, as well as to the engine's compressor pressure ratio $\pi_c^* = \dfrac{p_2^*}{p_1^*}$. According to the compressor universal characteristics, for a steady state engine regime, the air flow-rate depends on the pressure ratio and on the engine's speed $Q_a = Q_a\left(\pi_c^*, n\right)$ (Soicescu&Rotaru, 1999). The air flow-rate must be correlated to the fuel flow rate Q_i, in order to keep the optimum ratio of these values. When the correlation is not realized, for example when the fuel flow rate grows faster/slower than the necessary air flow rate during a dynamic regime (e.g. engine acceleration/deceleration), the corrector should modify the growing speed of the fuel flow rate, in order to re-correlate it with the realized air flow rate growing speed.

Modern engines' compressors have significant values of the pressure ratio, from 10 to 30, so the pressure difference $p_2^* - p_1^*$ could damage, even destroy, the transducer's elastic membrane and get it out of order. Thus, instead of p_2^*-pressure, an intermediate pressure p_f^*, from an intermediate compressor stage "f", should be used, the intermediate pressure ratio $\pi_f^* = \dfrac{p_f^*}{p_1^*}$ being proportional to π_c^*. The intermediate stage is chosen in order to obtain

a convenient value of p_f^*, around $4 \times p_1^*$. Both values of p_f^* and p_2^* are depending on compressor's speed (the same as the engine speed n), as the compressor's characteristic shows; consequently, the air flow rate depends on the above-mentioned pressure (or on the above defined π_c^* or π_f^*). The transducer's command chamber has two drossels, which are chosen in order to obtain critical flow through them (Soicescu&Rotaru, 1999), so the corrected pressure p_c^* is proportional to the input pressure:

$$p_c^* = \frac{S_{28}}{S_{29}} p_f^* \,, \tag{75}$$

where S_{28}, S_{29} are 28 and 29-drossels' effective area values. Consequently, the transducer operates like a π_c^*-based corrector, correlating the necessary fuel flow-rate with the compressor delivered air flow-rate. So, the corrector's equations are:

$$p_2^* = p_2^*(n) \text{ or } p_f^* = p_f^*(n), \tag{76}$$

and become, after transformations,

$$\overline{p_f^*} = k_{fn}\overline{n} \,, \tag{76'}$$

$$\overline{x_f} = k_\pi \overline{\pi_f^*} = k_{sf}\left(\overline{p_f^*} - \frac{1}{k_{1p}}\overline{p_1^*}\right). \tag{77}$$

The new form of (65)-equation becomes

$$S_R p_R - S_p p_p = m_s \frac{\mathrm{d}^2 y}{\mathrm{d}t^2} + \xi \frac{\mathrm{d}y}{\mathrm{d}t} + (k_{r1} + k_{r2})y - S_{mp}\left(p_c^* - p_1^*\right)\frac{l_6}{l_2} \,, \tag{78}$$

where S_{mp} is the transducer's membrane surface area. After linearization and Laplace transformer applying, its new non-dimensional form becomes

$$\left(T_y^2 s^2 + 2\omega_0 T_y s + 1\right)\overline{y} = k_{yR}\overline{p_R} - k_{yp}\overline{p_p} - \left(k_{tf}\overline{p_f^*} - k_{1t}\overline{p_1^*}\right), \tag{79}$$

where

$$k_{fn} = \left(\frac{\partial p_f^*}{\partial n}\right)_0 \frac{n_0}{p_{f0}^*} \,, k_\pi = \frac{S_{28}}{S_{29}} \frac{S_{mp}p_{f0}^*}{x_{f0}k_{r26}}\pi_{fr}^* \,, k_{tf} = \frac{S_{mp}p_{f0}^* k_{sf}}{(k_{r1}+k_{r2})y_0}\frac{l_6}{l_2} \,, k_{1t} = \frac{S_{mp}p_{10}^* k_{s\pi}}{(k_{r1}+k_{r2})k_{1p}y_0}\frac{l_6}{l_2} \,. \tag{80}$$

For a controller with both of the correctors, the (13)-lever equation results overlapping (73) and (79)-equations, which leads to a new form

$$k_{yR}\overline{p_R} - k_{yp}\overline{p_p} - k_{yH}\overline{p_1^*} - \left(k_{tf}\overline{p_f^*} - k_{1t}\overline{p_1^*}\right) = \left(T_y^2 s^2 + 2\omega_0 T_y s + 1\right)\overline{y} \cong \overline{y} \,, \tag{81}$$

which should replace the (65)-equation in the mathematical model (equations (63) to (69)). The new block diagram with transfer functions is depicted in figure 11.

5.3.4 System's quality

System's behavior was studied comparing the step responses of a basic controller and the step response (same conditions) of a controller with correctors. Fig. 15.a presents the step responses for a controller with barometric corrector, when the engine's regime is kept constant and the flight regime receives a step modifying. The differential pressure $\overline{p_d}$ becomes non-periodic, but its static error grows, from -0.1% to 0.77% and changes its sign. The profiled needle position y behavior is clearly periodic, with a significant override, more pulsations and a much bigger static error (1.85%, than 0.2%). Engine's most important output parameter, the speed n, presents the most significant changes: it becomes non-periodic (or remains periodic but has a short time smaller override), its static error decreases, from 1.1% to 0.21% and it becomes negative.

However, in spite of the above described output parameter behavior changes, the barometric corrector has realized its purpose: to keep (nearly) constant the engine's speed when the throttle has the same position, even if the flight regime (flight altitude or/and airspeed) significantly changes.

Figure 15.b presents system's behavior when an air flow-rate corrector assists the controller's operation. The differential pressure keeps its periodic behavior, but the profiled needle's displacement tends to stabilize non-periodic, which is an important improvement. The main output non-dimensional parameters, the engine's speed $\overline{n}$ and the combustor's temperature $\overline{T_3^*}$ have suffered significant changes, comparing to figure 14.b; both of them tend to become non-periodic, their static errors (absolute values) being smaller (especially for $\overline{n}$). System's time of stabilization became smaller (nearly half of the basic controller initial value). So, the flow rate corrector has improved the system, eliminating the overrides (potential engine's overheat and/or overspeed), resulting a non-periodic stable system, with acceptable static errors (5.5% for $\overline{n}$, 3% for $\overline{T_3^*}$) and acceptable response times (5 to 12 sec).
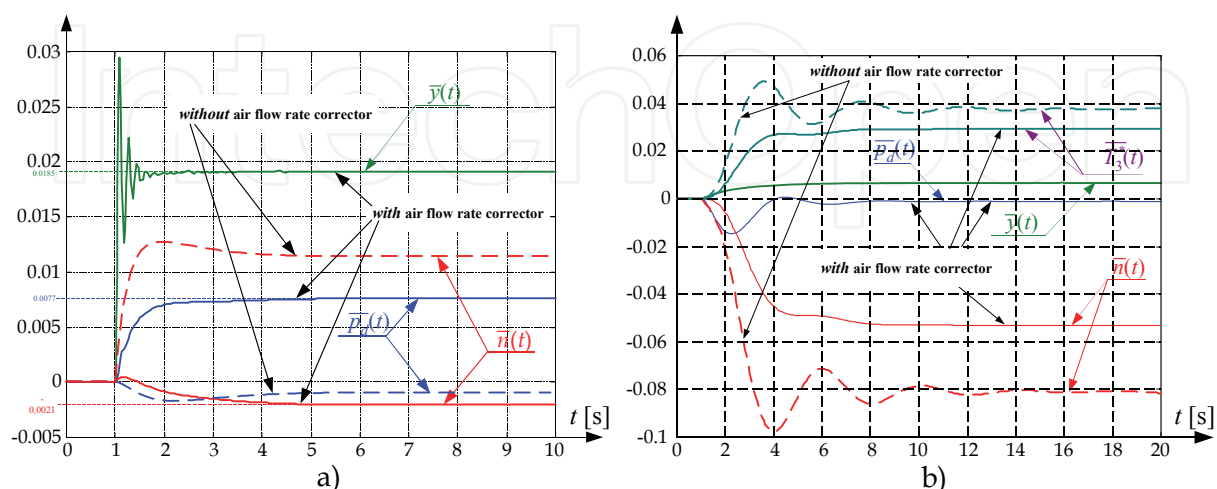

Fig. 15. Compared step response between a basic controller and a controller with
a) barometric corrector, b) air flow rate corrector

The barometric corrector is simply built, consisting of two capsules; its integration into the controller's ensemble is also accessible and its using results, from the engine's speed point of view, are definitely positives; new system's step response shows an improvement, the engine's speed having smaller static errors and a faster stabilization, when the flight regime changes. However, an inconvenience occurs, short time vibrations of the profiled needle (see figure 15.b, curve $\bar{y}(t)$), without any negative effects above the other output parameters, but with a possible accelerated actuator piston's wearing out.

The air flow rate corrector, in fact the pressure ratio corrector, is not so simply built, because of the drossels diameter's choice, correlated to its membrane and its spring elastic properties. However, it has a simple shape, consisting of simple and reliable parts and its operating is safe, as long as the drossels and the mobile parts are not damaged.

Air flow-rate corrector's using is more spectacular, especially for the unstable engines and/or for the periodic-stable controller assisted engines; system's dynamic quality changes (its step response becomes non-periodic, its response time becomes significantly smaller).

6. Conclusions

Fuel injection is the most powerful mean to control an engine, particularly an aircraft jet engine, the fuel flow rate being the most important input parameter of a control system.

Nowadays hydro-mechanical and/or electro-hydro-mechanical injection controllers are designed and manufactured according to the fuel injection principles; they are accomplishing the fuel flow rate control by controlling the injection pressure (or differential pressure) or/and the dosage valve effective dimension.

Studied controllers, similar to some in use aircraft engine fuel controllers, even if they operate properly at their design regime, flight regime's modification, as well as transient engine's regimes, induce them significant errors; therefore, one can improve them by adding properly some corrector systems (barometric and/or pneumatic), which gives more stability an reliability for the whole system (engine-fuel pump-controller).

Both of above-presented correctors could be used for other fuel injection controllers and/or engine speed controllers (for example for the controller with constant pressure chamber), if one chooses an appropriate integration mode and appropriate design parameters.

7. References

Abraham, R. H. (1986). *Complex dynamical systems,* Aerial Press, ISBN #0-942344-27-8, Santa Cruz, California, USA

Aron, I.; Tudosie, A. (2001). Jet Engine Exhaust Nozzle's Automatic Control System, *Proceedings of the 17th International Symposium on Naval and Marine Education*, pp. 36-45, section III, Constanta, Romania, May 24-26, 2001

Jaw, L. C.; Mattingly, J. D. (2009). *Aircraft Engine Controls:Design System Analysis and Health Monitoring,* Published by AIAA, ISBN-13: 978-1-60086-705-7, USA

Lungu, R.; Tudosie, A. (1997). Single Jet Engine Speed Control System Based on Fuel Flow Rate Control, *Proceedings of the XXVIIth International Conference of Technical Military Academy in Bucuresti*, pp. 74-80, section 4, Bucuresti, Romania, Nov. 13-14, 1997

Lungu, R. (2000). *Flying Vehicles Automation,* Universitaria, ISBN 973-8043-11-5, Craiova, Romania

Mattingly, J. D. (1996). *Elements of Gas Turbine Propulsion,* McGraw Hill, ISBN 1-56347-779-3, New York, USA

Moir, I.; Seabridge, A. (2008). *Aircraft Systems. Mechanical, Electrical and Avionics Subsystems Integration,* Professional Engineering Publication, ISBN-13: 978-1-56347-952-6, USA

Stoenciu, D. (1986). *Aircraft Engine Automation. Catalog of Automation Schemes,* Military Technical Academy Printing House, Bucuresti, Romania

Stoicescu, M.; Rotaru, C. (1999). *Turbo-Jet Engines. Characteristics and Control Methods,* Military Technical Academy Printing House, ISBN 973-98940-5-4, Bucuresti, Romania

Tudosie, A. N. (2009). Fuel Injection Controller with Barometric and Air Flow Rate Correctors, *Proceedings of the WSEAS International Conference on System Science and Simulation in Engineering* (ICOSSSE'09), pp. 113-118, ISBN 978-960-474-131-1, ISSN 1790-2769, Genova, Italy, October 17-19, 2009.
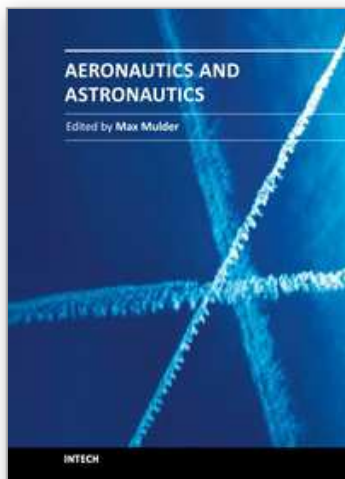
Aeronautics and Astronautics

Edited by Prof. Max Mulder

ISBN 978-953-307-473-3

Hard cover, 610 pages

Publisher InTech

Published online 12, September, 2011

Published in print edition September, 2011

In its first centennial, aerospace has matured from a pioneering activity to an indispensable enabler of our daily life activities. In the next twenty to thirty years, aerospace will face a tremendous challenge - the development of flying objects that do not depend on fossil fuels. The twenty-three chapters in this book capture some of the new technologies and methods that are currently being developed to enable sustainable air transport and space flight. It clearly illustrates the multi-disciplinary character of aerospace engineering, and the fact that the challenges of air transportation and space missions continue to call for the most innovative solutions and daring concepts.

INTECH
open science | open minds